Corrosion Science 112 (2016) 233–240

Contents lists available at ScienceDirect

Corrosion Science

journal homepage: www.elsevier.com/locate/corsci

Pitting corrosion of martensitic stainless steel in halide bearing solutions

S. Pahlavan, S. Moazen, I. Taji, K. Saffar, M. Hamrah, M.H. Moayed*, S. Mollazadeh Beidokhti

Metallurgical and Material Engineering Department, Faculty of Engineering, Ferdowsi University of Mashhad, Mashhad 91775-1111, Iran

ARTICLE INFO

Article history:
Received 8 December 2015
Received in revised form 23 May 2016
Accepted 9 July 2016
Available online 15 July 2016

Keywords:
A. Stainless steel
B. Polarisation
B. Potentiostatic
C. Pitting corrosion

ABSTRACT

In this research, pitting corrosion of martensitic stainless steel in presence of halide anions was investigated by using polarization techniques. Results confirm that the aggressivity of halides increases in the following order: $I^- < Br^- < Cl^-$. Although fluoride does not offer any pitting by itself, its presence together with chloride increases the occurrence frequency of metastable pits and pitting potential, simultaneously. While the pitting was more probable in NaCl solution, its metastable stability product was observed equal or even less than other solutions.

1. Introduction

Nowadays, stainless steels are widely utilized in industry due to their proper resistance to corrosion alongside with their high strength. They owe their corrosion resistance to the presence of at least 12% Cr in their composition [1]. This kind of composition causes the formation of adherent passive film which impedes the corrosion of substrate metal. However, the passive film formed on stainless steels has some weak points such as inclusions, grain boundaries and other discontinuities through which aggressive ions can develop a localized breakdown and consequently the pitting corrosion [2–8]. There are three distinct stages in pitting; nucleation, metastable pitting and stable growth. Aggressive anions are effective in both initiation and propagation of pits [2,3,9,10].

Numerous aggressive anions have been reported for various alloys. Of these aggressive anions, halides are the most important group which provoke localized corrosion for a lot of metals and alloys such as stainless steels, aluminium and zinc [3,11–13]. Nevertheless, conducted researches about iodide and bromide are much less than chloride. The studies about the effect of these three anions show that the pitting potential of iron and stainless steels has the most value for iodide and the lowest one for chloride [14–16]. It has also been reported that fluoride ions do not induce localized corrosion attack in stainless steels [16]. Pardo et al. [17] found that the presence of fluoride anions, together with chloride anions favours the pitting for both superduplex and superaustenitic stainless steels. Bastidas et al. reported the formation of some small pits on S32550 SS in mixed chloride and fluoride aqueous solution. The morphology of these pits was cavernous and hemispherical pits were not found [18]. On the other hand, Yamazaki's investigations showed that the effect of increasing F^- in NaCl solution is to raise the crevice corrosion potential [19]. Kaneko and Isaacs also studied the effect of molybdenum on the pitting of ferritic stainless steels in chloride and bromide bearing solutions. They found that Mo has a strong positive effect on pitting, but the effect is more dramatic in the case of chloride [20]. They also found that increasing the relative concentration of bromide in mixed solutions of chloride and bromide, raises the pitting potential [21].

Stainless steels are commonly divided into five groups including: austenitic, ferritic, martensitic, duplex and precipitation hardening [1,22]. The martensitic group has the highest strength but also the lowest corrosion resistance. Even so, because of their strength, hardness and fairly good corrosion resistance, they are utilized as tool and cutlery alloys, mining equipment and compressor blades [1,22–25].

In this study the effect of different halide anions on the pitting initiation and propagation of 403 martensitic stainless steel (SS) was examined. Cr is the main alloying element in 403 martensitic SS which is necessary for being stainless. Plus, some additional proofs describing the effect of fluoride on pitting were also made by using

* Corresponding author.
E-mail address: mhmoayed@um.ac.ir (M.H. Moayed).

http://dx.doi.org/10.1016/j.corsci.2016.07.008
0010-938X/

Table 1
Chemical composition (wt%) of studied 403 martensitic stainless steel.

C	Cr	Ni	Mn	Si	Cu	Mo	N	Co	V	P	S	Other	Fe
0.165	11.64	1.00	0.83	0.29	0.16	0.04	0.04	0.04	0.03	0.03	0.01	>0.01	Bal.

the wire of 17-4PH martensitic SS. Investigations were sought by using potentiodynamic and potentiostatic polarizations.

2. Experimental procedures

2.1. Materials and preparations

Main experiments were performed on 403 martensitic stainless steel. The composition of the alloy has been represented in Table 1. The exposed surfaces in potentiodynamic and potentiostatic tests were 1 and 0.25 cm^2, respectively. All specimens were solution annealed at 1050 °C for 1 h and cooled in air. Afterwards, tempering was conducted at 300 °C for 1 h and cooled again in air. Surfaces of working electrodes were prepared by grinding up to 1200 SiC paper. In order to diminish the possibility of crevice corrosion occurrence [26,27], samples were prepassivated in the 0.1 M Na_2SO_4 solution by applying the constant potential of 850 mV (SCE) for 1800 s. Samples were then mounted in an inert epoxy resin. Prior to each test the exposed surface of specimen was washed by deionized water and dried by flowing warm air. For some additional proofs, wire of 17-4PH SS was also served as the pencil electrode. Its chemical composition was contained 0.04% C, 0.012% S, 0.018% P, 0.32% Si, 0.61% Mn, 4.14% Cu, 4.59% Ni, 15.09% Cr, 0.013% V, 0.358% Nb and 0.18% Mo.

2.2. Potentiodynamic experiments

Potentiodynamic experiments were carried out in three-electrode cell at sweep rate of 30 mV/min. A saturated calomel electrode (SCE) and a platinum plate served as reference and auxiliary electrodes, respectively. For all experiments, open circuit potential was measured 1 h prior to the polarization, which was enough to approach the steady state condition. All experiments were performed at room temperature and were repeated thrice to check their reproducibility.

Experiments were carried out in solutions of NaF, NaCl, NaBr, NaI and mixed solutions of NaF and NaCl. Mixed solutions were studied to identify the interactive effect of fluoride and chloride. All test solutions were prepared from reagent grade chemicals and deionized water and concentrations were also chosen based on the need. The electrochemical cell was a 250 ml beaker open to the air.

Apart from main experiments, the role of fluoride ion on the pitting was also studied by additional potentiodynamic tests carried out on artificial pits of 17-4PH stainless steel. The wire was mounted in an epoxy resin and has the diameter of 70 μm. Prior to each test OCP potential was recorded for 15 min to achieve the steady state condition. Experiments were performed in solutions of 1 M HCl and 0.5 M HF + 0.5 M HCl. It must be noted that for better comparison, the pHs of two latter solutions were also measured by pH meter.

2.3. Potentiostatic experiments

To investigate metastable pitting, potentiostatic experiments were performed at constant potential of −50 mV (SCE) for 900 s. Before running the test, corrosion potential was recorded for 10 min. Experiments were repeated thrice at room temperature in the following solutions: 0.5 M NaI, 0.5 M NaBr, 0.5 M NaCl and 0.5 M NaF + 0.5 M NaCl. To inquire into the synergetic effect of fluoride alongside with the chloride, injection experiments were also carried out. Potentiostatic tests were performed for chloride bearing solution and fluoride ion was injected into the solution at 500th second. This test was also repeated for fluoride bearing solution and this time chloride was injected into it.

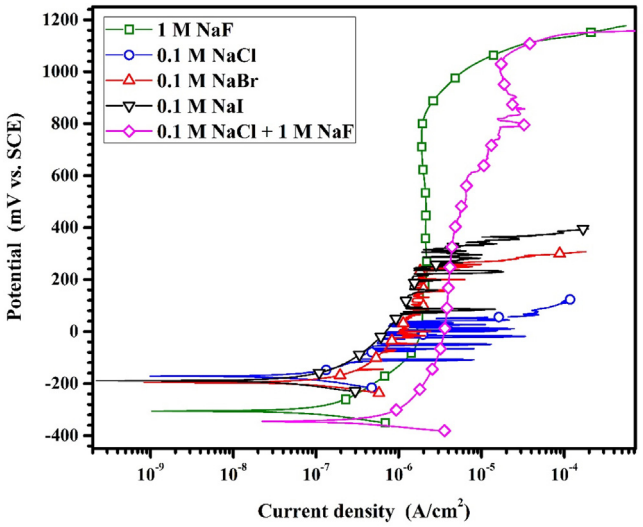

Fig. 1. Typical potentiodynamic curves for typical studied solutions.

3. Results

3.1. Breakdown potential

Typical potentiodynamic polarization curves obtained in solutions of NaI, NaBr, NaCl, NaF and mixed solutions of NaF and NaCl are depicted in Fig. 1. There is no noticeable change in the corrosion potential. Passivity current for fluoride bearing solutions has the more value compared with NaCl, NaBr and NaI. Abundant metastable pits are also visible in potentiodynamic curves of NaCl, NaBr and NaI solutions.

Typical potentiodynamic curve for 1 M NaF solution shows that fluoride does not provoke localized corrosion even in the highest studied concentration and the potentiodynamic curve continues up to high potentials without any pitting. A typical potentiodynamic curve for 0.1 M NaCl + 1 M NaF solution is also shown in Fig. 1, however after the test the specimen surface was highly pitted. To distinguish between pitting and transpassivity in fluoride bearing solutions, plus the visual examination, the reverse sweep was conducted at the current density of 0.3 mA/cm^2. No pit was observed on the sample visually for 1 M NaF solution and the reverse-sweep of potential also regressed on upward potential sweep which confirms that the case is not the pitting. These two methods were also used for mixed solutions of NaF and NaCl and the pitting was recognized in all relative concentrations of fluoride. Fig. 2 schematically shows the difference of reverse-sweep curves after the pitting and the transpassivity. Indeed, Fig. 3 also depicts some of the pits observed on the specimen surface after the polarization (upward and reverse sweep) in 0.1 M NaCl + 1 M NaF solution.

In general, pitting is a probabilistic and statistical phenomenon, so that different conditions of experiment can influence the E_{pit} [28,29]. Therefore, every experiment was repeated thrice and the mean value of E_{pit} was then reported. These mean values are indi-

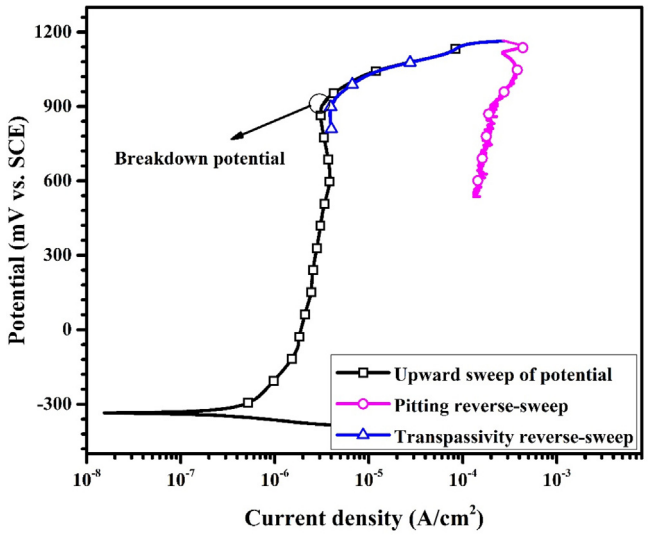

Fig. 2. The schematic illustration shows how the pitting was distinguished from transpassivity in potentiodynamic experiments. The point regarded as breakdown potential in all potentiodynamic test has also been included, exemplary.

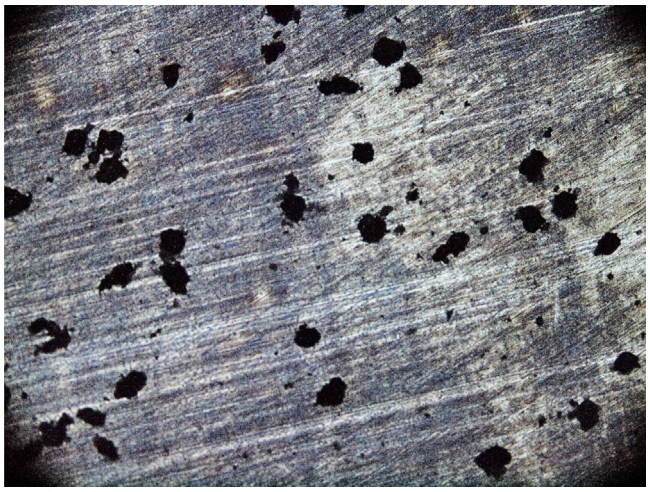

Fig. 3. Some pits observed (20× by optic microscope) on the specimen surface in the solution of 0.1 M NaCl + 1 M NaF. The imaging was conducted after upward potential sweep and reverse sweep at 0.3 mA/cm^2.

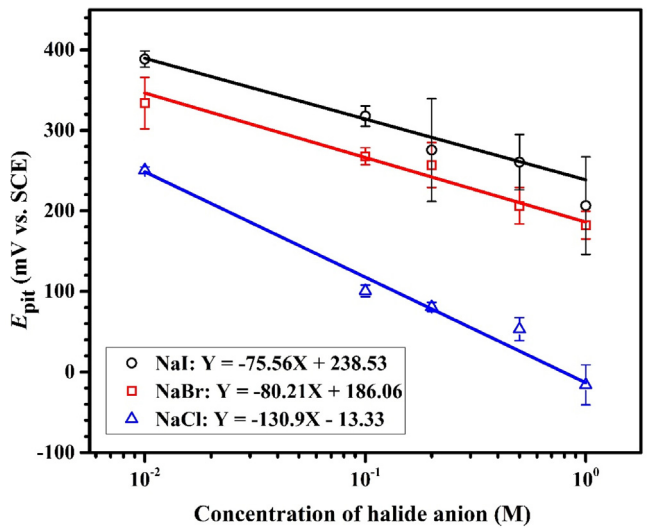

Fig. 4. Pitting potential for 5 different concentrations of NaCl, NaBr and NaI and the linear fitting of the curves. Error bars represent 95% confidence limits measured from three experimental tests under identical conditions.

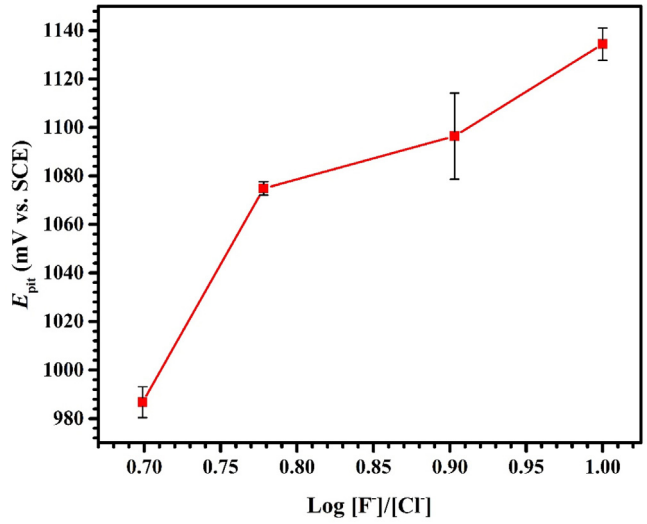

Fig. 5. Pitting potentials obtained in mixed solutions of NaF and NaCl. The inhibition effect of fluoride is obvious in the case of 403 martensitic SS.

cated in Fig. 4 for various studied concentrations of NaCl, NaBr and NaI. Considering Fig. 4 it can be said that there is a linear relationship between the pitting potential and the concentration of the aggressive ion, as it is also reported by other authors [3,10,30,31]. Eq. (1) is given based on their works and describes this linear relationship:

$$E_{pit} = A - B \log C_x \quad (1)$$

where A and B are constants, C_x is the concentration of the aggressive ion and E_{pit} is the pitting potential. In this study the constant B was calculated 130 mV/decade for chloride bearing system, although it is reported that it varies between 50 and 100 mV/decade [31]. As it is shown in Fig. 4, for each concentration, the pitting potential has the lowest value in NaCl and has the highest value in NaI. It can also be seen that the absolute slope of the lines increases in the following order: NaCl > NaBr > NaI.

The behaviour of F^- which is also illustrated in Fig. 5 imparts that the fluoride has the inhibition effect in the case of pitting corrosion. In Fig. 5 pitting potential is plotted versus the logarithm of the relative concentration of fluoride and chloride. Fluoride, being present alongside the chloride, increases the pitting potential.

3.2. Metastable growth

Fig. 6a is the result of a potentiostatic polarization in which the constant potential of −50 mV (SCE) was applied to the specimen immersed in solution of 0.5 M NaBr. The decrement of the current density in the first seconds of recording is due to the formation of the passive film. After a while, current density decreases to a constant passivity current density and becomes stable. There are many transients lay over the background current which are characterized as the metastable pits. As the pit nucleates and begins to grow, the current density increases from the passivity background, because of dissolution of metal. After a short time of growth, the cover over the pit mouth ruptures and the pit solution dilutes. Consequently, the metastable pit repassivates and the current density falls to passivity at once [9,32–35]. Fig. 6b schematically shows one of these metastable pits for which different quantities can be defined. Of these quantities, lifetime, peak current (I_{peak}) and dissolved charge

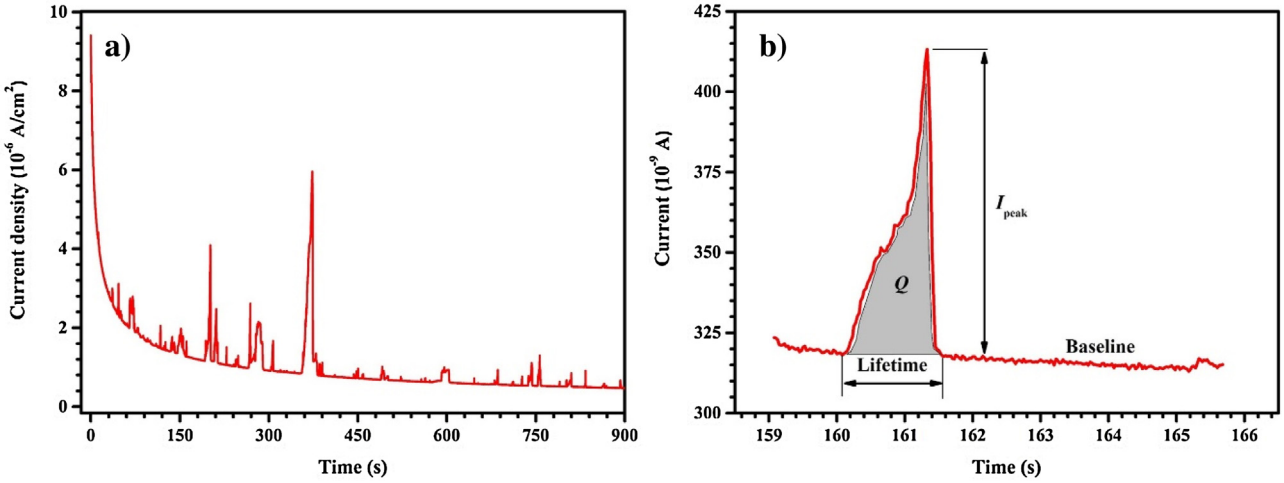

Fig. 6. (a) A typical current density transients obtained from potentiostatic polarization of the specimen in solution of 0.5 M NaBr. The employed constant potential is −50 mV (SCE) and the current density is recorded for 15 min. (b) a typical metastable pit obtained from the latter figure and some of its corresponding quantities. Data acquisition rate: 40 Hz.

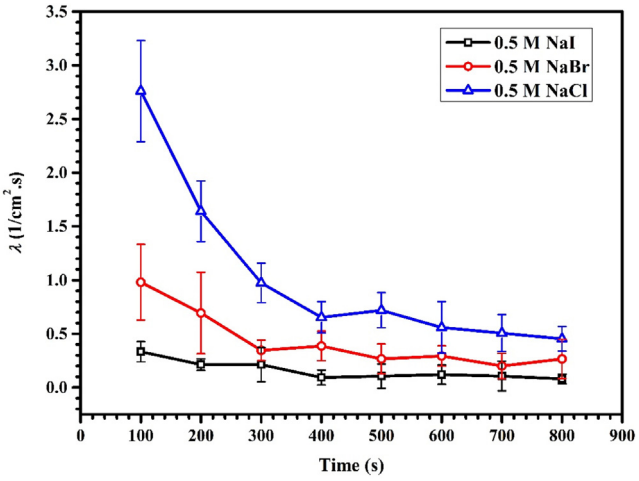

Fig. 7. The frequency of occurrence of metastable pits for 0.5 M solutions of NaI, NaBr and NaCl. The values have obtained at the constant potential of −50 mV (SCE). Error bars represent 95% confidence limits measured from three experimental tests under identical conditions.

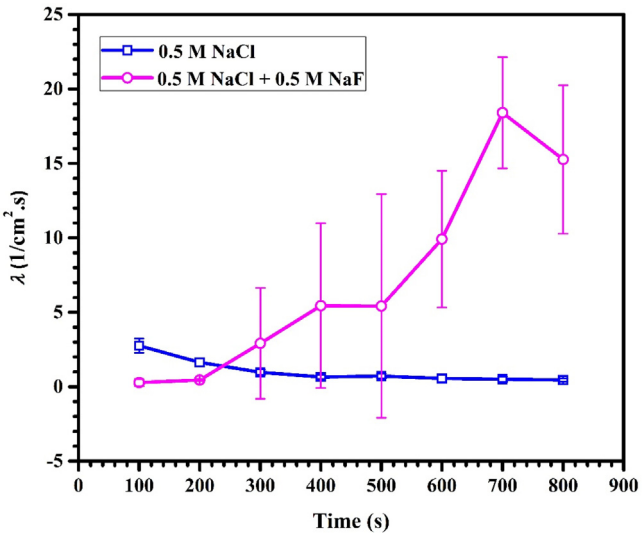

Fig. 8. The frequency of occurrence of metastable pits for 0.5 M NaCl and 0.5 M NaF + 0.5 M NaCl. The values have obtained at the constant potential of −50 mV (SCE). Error bars represent 95% confidence limits measured from three experimental tests under identical conditions.

(Q) have been shown in the figure. It should be noted that the current density has been turned into current in Fig. 6b by multiplying to exposed surface area. Q is achieved by integrating the current-time curve and then the pit depth of hemisphere-assumed pits is calculated by applying Faraday's second law, as follows:

$$r = \left(\frac{3ZQ}{2\pi nF\rho}\right)^{\frac{1}{3}} \quad (2)$$

where r represents the hemisphere radius, Q is the dissolved charge, Z is the molar mass and ρ is the density. n and F are also the number of involved electrons and Faraday's constant, respectively.

Fig. 7 illustrates the occurrence frequency of metastable pits, λ, for 0.5 M solutions of NaCl, NaBr and NaI. λ is defined as the total number of metastable pits initiated per unit area in 100 s obtained by potentiostatic experiments. As shown in Fig. 6a no transients are unfolded in the first seconds of the experiment because of high current density. Thus, first 50 s of each experiment was wiped out and eight 100-s intervals were then chosen for calculating λ. As it can be seen, λ has a downward trend for all three lines which belongs to Cl, Br and I. The downward trend is due to diminishing the preferred sites for nucleation of pits [9].

Fig. 8 compares the occurrence frequency of metastable pits for 0.5 M NaCl and 0.5 M NaF + 0.5 M NaCl. It is observable that presence of fluoride has strongly raised the total number of metastable pits. The more important point is that λ increases by time despite the reason quoted above.

Fig. 9 illustrates the cumulative distribution of metastable pits lifetime for the following solutions: 0.5 M NaI, 0.5 M NaBr, 0.5 M NaCl and 0.5 M NaF + 0.5 M NaCl. The lifetime is taken as the difference between the moment at which the current begins to increase and the moment it decreases and reaches to the baseline current. The horizontal axis in this graph is the lifetime and the vertical axis is the probability function defined as:

$$P(t) = \frac{n}{1+N} \quad (3)$$

where N is the total number of events and n is the number of event. To compare the lifetime of metastable pits in different solutions, median value of $P(t)$ can be chosen, i.e. $P(t) = 0.5$. As Fig. 9 shows, metastable pits have the longest lifetime in the NaI solution and the shortest lifetime belongs to the mixed solution of NaF and NaCl.

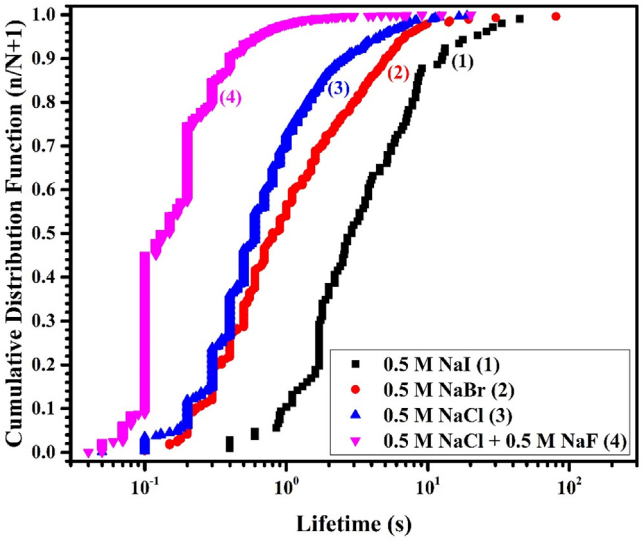

Fig. 9. The cumulative distribution of metastable pits lifetime for different solutions containing halide anions.

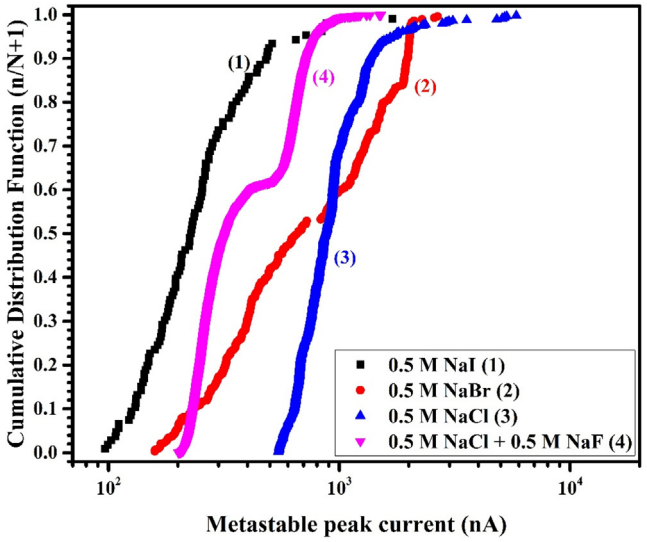

Fig. 11. The cumulative distribution of metastable pits peak currents for different solutions containing halide anions.

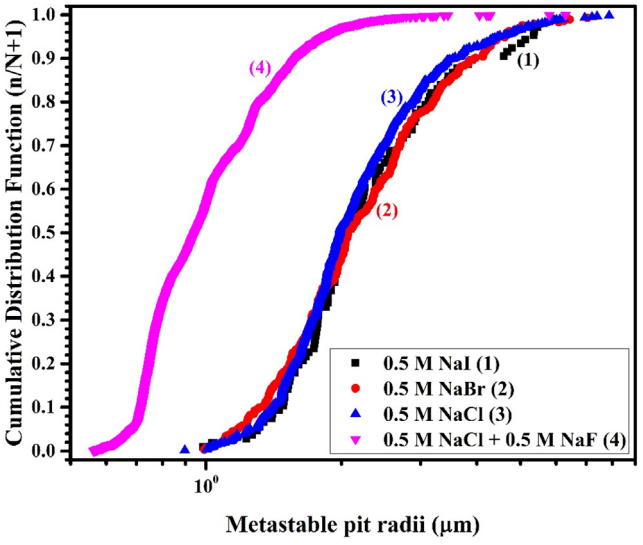

Fig. 10. The cumulative distribution of metastable pits radii for different solutions containing halide anions.

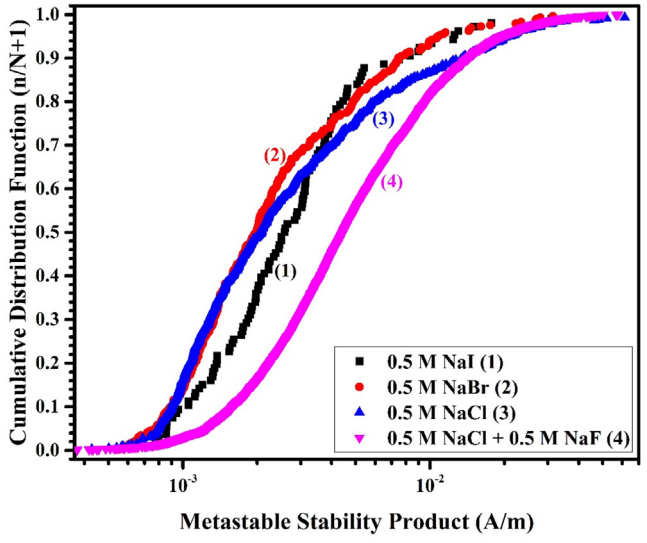

Fig. 12. The cumulative distribution of metastable pits stability product for different solutions containing halide anions.

Metastable pits lifetime in NaBr and NaCl are also 0.8 s and 0.6 s, respectively. Pitting is less probable in NaI solution, but the lifetime of metastable pits is the longest one among studied halides.

Fig. 10 shows the cumulative distribution of calculated metastable pit radii (r_{pit}) for different solutions. As it can be seen, metastable pit radii have a very similar distribution in NaI, NaBr and NaCl solutions, so that the median value of pit radius is nearly 2 μm for all of them. The smallest pit radius although, is approximately 0.945 μm and belongs to mixed solution of NaF and NaCl. In the other word, the presence of fluoride alongside with the chloride has decreased the pit radius approximately 1 μm.

The cumulative distribution of metastable pit peak current has been depicted in Fig. 11. Evidently, the lowest metastable peak current belongs to NaI solution. The median value of metastable peak current for NaCl and NaBr solutions are close together, with wider deviation in the case of NaBr solution. It can also be seen that the fluoride presence alongside with the chloride has caused the metastable peak current to decrease about 500 nA.

Galvele [9] has proposed a criterion to determine the stability probability of a metastable pit. This criterion is called stability product and defined as the product of pit current density, *i*, and the pit depth, *a*. If the stability product of a metastable pit exceeds the critical value, the pit will become stable. Fig. 12 shows the cumulative distribution of metastable pits stability product. According to the figure the metastable stability product increases in the following order: NaBr < NaCl < NaI < NaF + NaCl. Presence of the fluoride alongside with the chloride has approximately doubled the stability product value compared with sole NaCl solution. The median values for NaI, NaBr and NaCl are 0.026 mA/cm, 0.020 mA/cm and 0.021 mA/cm, respectively.

3.3. The synergistic effect of fluoride

To inquire into the effect of fluoride on the pitting, aggressive anion injection potentiostatic experiments were carried out in which fluoride was injected into the chloride bearing solution and vice versa. Fig. 13 compares potentiostatic injection exper-

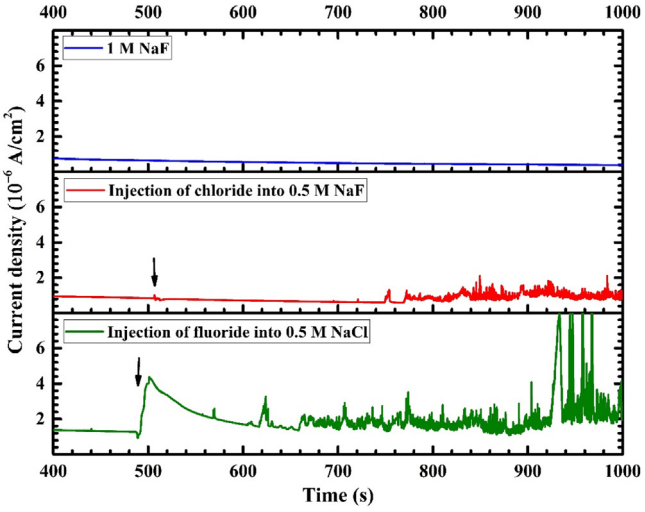

Fig. 13. Comparison of typical potentiostatic experiments conducted in NaF solution and injection cases in which chloride injected to NaF and fluoride injected to NaCl solutions. The final concentration of the injection cases was 0.5 M NaF + 0.5 M NaCl. Arrows are indicating the injection time. Data acquisition rate: 40 Hz.

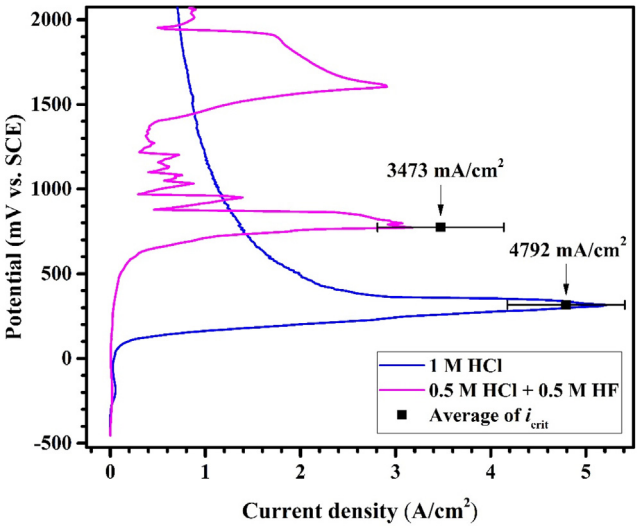

Fig. 14. Typical potentiodynamic tests conducted by 17-4PH pencil electrode in 1 M HCl and 0.5 M HCl + 0.5 M HF solutions. Averages of critical current densities have been shown and error bars represent 95% confidence limits measured from three experimental tests under identical conditions.

iments conducted for 1 M NaF and mixed solutions of NaF and NaCl. As can be seen, there is no metastable pitting in sole NaF solution. In the second case, chloride was injected into the solution of 0.5 M NaF at 500th second. The concentration of solution was finally reached 0.5 M NaF + 0.5 M NaCl. The employed constant potential was −50 mV (SCE) similar to previous tests. By adding fluoride in chloride bearing solution, the occurrence of metastable pits severely increases after an incubation time of about 220 s.

The third case is about the injection of fluoride into the chloride bearing solution with identical conditions. By injection the fluoride into the chloride bearing solution the metastable pits occurrence has also become abundant after a lower incubation time (around 100 s). In addition, metastable pits have higher currents in this situation in comparison with the second one.

3.4. The inhibition effect of fluoride

More inspection on the inhibition effect of fluoride was conducted by assessment of critical current density necessary for passivity (i_{crit}) in acidic solutions containing fluoride and chloride. Potentiodynamic polarizations were performed by pencil electrode in 1 M HCl and 0.5 M HCl + 0.5 M HF solutions. The two mentioned solutions have the similar molarity of protons, if dissociation takes place completely. So it can be easily investigated that how the fluoride influences the i_{crit}. Fig. 14 illustrates typical potentiodynamic polarizations for 17-4PH SS pencil electrode in the two considered solutions. The chemical composition of 17-4PH electrode was similar to 403 martensitic SS except in the case of Ni and Cu which do not participate in the composition of pit solution [36]. As Fig. 14 shows, the critical potential of fluoride is higher than that for chloride. In addition, fluoride has reduced i_{crit} compared with chloride. The measured pHs after 12 h for 1 M HCl and 0.5 M HCl + 0.5 M HF were 0.9 and 1.3, respectively. After attaining the passivity, there are again some fluctuations in fluoride bearing solution. It shows that the passivity in mixed solution of NaF and NaCl is not as stable as sole NaCl solution.

4. Discussion

4.1. Stable pitting

Pitting potential (E_{pit}) is considered as the potential at which current density increases sharply without regression. Results (Figs. 1, 4 and 5) reveal that E_{pit} in chloride containing solution has the lowest value among halide ions and has the most one for iodide. Consequently, it can be said that chloride has the most aggressivity among the halides. No pitting was however detected in sole fluoride bearing solutions in the case of 403 martensitic SS. Polarization curves obtained in mixed solutions of NaF and NaCl nevertheless, demonstrate an inhibition effect for fluoride, so that the pitting potential of 403 martensitic SS, rises by increasing the relative concentration of fluoride.

Considering the passivity current in all halide bearing solutions (Fig. 1), it can be concluded that the passivity current is probably affected by ionic radius of halides. The passivity current in halide bearing solutions increases in the following order: NaI < NaBr < NaCl < NaF. Increment of passivity current in mixed solution of NaF and NaCl may also confirms that the presence of fluoride alongside with the chloride, weakens the formed passive layer.

4.2. Metastable pitting

Metastable pits are also obvious in potentiodynamic curves for NaCl, NaBr and NaI, as the transients prior to the pitting potential, but there are no transients in the case of fluoride. It is observable in Fig. 1 that the quantity of metastable pits increases from iodide to chloride. These metastable pits are also obvious in the mixed solutions of NaF and NaCl.

On the other hand, statistical calculations show that for NaCl, NaBr and NaI solutions, the occurrence frequency of metastable pits decreases by the time due to diminishing of the preferred sites for pit nucleation [9]. Considering the existing mechanisms, the ionic radius of species plays an important role in nucleation. The smaller the ionic radius, the more activity in nucleation step of pitting [37]. So, according to Fig. 7, as the ionic radius increases in the order: $Cl^- < Br^- < I^-$, the number of initiated metastable pits decreases. Of these three, chloride is the most active ion in the initiation step of

Table 2
Comparison the pK_a of four hydrohalic acids [38].

Hydrohalic acid	HF	HCl	HBr	HI
Acidity ($-pK_a$)	3	−7	−9	−10

pitting and its corresponding λ has the most value in all intervals. NaBr and NaI solutions are situated after the NaCl, respectively. It was observed that presence of fluoride has strongly raises the total number of metastable pits and increases λ by time despite reasons quoted above (Fig. 8). According to initiation mechanisms, the smaller ionic radius of fluoride can promote the nucleation of metastable pits in mixed solutions of NaF and NaCl. Now, there is a question and that is, if the fluoride promotes the metastable pitting alongside with the chloride, why there is no metastable pit in NaF solution itself? The answer may back to the inactivity of fluoride in propagation step of pitting.

According to the acidification theory [10], after the initiation of a pit, anions migrate into it. If these anions unite with protons produced by hydrolysis of dissolved metal cations, the pH of pit solution increases and pitting will be impeded. So, the pitting will be related to the pK_a. The pK_as for hydrohalics have been represented in Table 2. It can be said now, being a component of weak acid, F^- has very high tendency to form a bond with H^+ and form a thermodynamically stable HF. Thus, an initiated pit cannot propagate in presence of sole fluoride, because it consumes almost all protons. Or maybe it is better to say that the propagation in this case may be such low which was not detected in conducted experiments. The high passivity current in NaF solution can be a proof for large number of initiated pits weakening the passive layer. The high density of initiated pits in NaF solution might cause the passivity current to increase, even to higher values in comparison with NaCl solution. It may be concluded that duo to the lower value of current transients compared with electrical noise of measuring instrument the metastable pits of the stainless steel in NaF solution cannot be detected. Considering the Table 2, other halides promote the pitting propagation, because of their low pK_as which is low enough to acidify the pit solution.

All the median values for the cumulative distributions obtained by statistical experiments (shown in Figs. 9–12) have been listed in Table 3. Comprising the NaCl, NaBr and NaI solutions, it can be said that the metastable pit growth rate decreases by increasing the anion radius, maybe because of the more difficult diffusion. According to the cumulative figures (Figs. 9–12) and the Table 3, metastable pit radii are similar in these three and their median values are all around 2 μm. Therefore, as the lifetime is the longest and the peak current is the lowest for NaI solution, it can be concluded that the metastable pits grow very lightly in iodide bearing solutions. In the case of NaCl solution, although, the inverse circumstance is valid, so that the shortest lifetime and the highest peak current among these three anions, indicate the fastest growth of metastable pits. The intermediate growth rate also pertains to the NaBr solution which approximately has the intermediate lifetime and peak current.

Besides, by comparison the cumulative figures for NaCl and NaF + NaCl solutions, it can be said that the fluoride presence alongside with the chloride has decreased the metastable growth. In the other word, fluoride do not let the metastable pit to grow more, by retarding the acidification.

4.3. Stability product

Distribution of the stability products obtained in different halide bearing solution also stresses that the highest metastable stability product does not necessarily belongs to the most susceptible system to pitting. In the other word and according to Fig. 12, although the pitting is less probable in NaI and NaBr solutions, their corresponding stability products are equal to NaCl solution, or even slightly higher in the case of iodide. The stability product of NaF + NaCl solution is higher than NaCl solution, while the pitting potential is lower in sole NaCl solution. This inconsistency may be because of the fact that the critical pit stability product is not equal in different solutions. In the other word, it is possible that the critical pit stability product is higher in NaI, NaBr and NaF + NaCl solutions.

4.4. Synergistic effect of fluoride

It was observed that fluoride increases the metastable pitting events being present alongside with chloride (Fig. 8). This synergistic effect of fluoride in increasing the occurrence frequency of metastable pits, also achieved in injection experiments (Fig. 13). Although the stainless steel remains passive in fluoride bearing solution, chloride injection into it causes metastable pitting to occur, intensively. Inversely, injection of fluoride into chloride bearing solution with the same concentration causes more severe metastable pitting, by a shorter incubation time. The shorter incubation time in this case, may back to the faster penetration of fluoride due to its smaller radius in comparison with chloride. Pit nucleation events in injection experiments are in accordance with occurrence frequency results shown in Fig. 8. The more activity of fluoride in initiation step of pitting and the action of chloride in propagation leads to detection of abundant metastable pitting events.

4.5. Inhibition effect of fluoride

It was mentioned that synergistic effect of fluoride which raises the occurrence frequency of metastable pits, is concomitant with an inhibition effect. This inhibition effect of fluoride causes the E_{pit} to raise (Fig. 5) and can be explained again by Galvele's acidification theory [10]. The rationale of this phenomenon is consuming the protons produced inside the pit. Fluoride because of its high pK_a, bonds with H^+, increases the pH and consequently retards the pitting. pH measurements also confirmed that fluoride increases the pH by interacting with protons. An alternative way to see this effect by pencil electrode studies (Fig. 14) also shows that fluoride lowers the critical current density obtained in 0.5 M HCl + 0.5 M HF solution. This decrement in critical current density can be attributed to the consumption of protons by fluoride. In the other word, consumption of protons in fluoride bearing solution causes the pit environment to become less harsh with higher pH value. Hence, the passivity is reached in lower current densities. It must be noted that it is not expected that the corrosion behaviour of 403 and 17-

Table 3
Median values of cumulative distribution for lifetime, pit radii, peak current and stability product obtained from different solutions.

Solution	Lifetime (s)	Pit radii (μm)	Peak current (nA)	Stability product (mA/cm)
0.5 M NaI	2.9	2.060	227.86	0.026
0.5 M NaBr	0.80	2.071	662.16	0.020
0.5 M NaCl	0.60	1.984	873.31	0.021
0.5 M NaF + 0.5 M NaCl	0.13	0.945	321.03	0.045

4PH SSs to be similar. The expected thing is further observation of the fluoride behaviour in consuming the protons in the case of wire of 17-4PH SS.

5. Conclusion

1. The values of pitting potential for halides confirm that aggressivity of them increases in the following order: $I^- < Br^- < Cl^-$.
2. Fluoride does not provoke pitting by itself, but its presence together with chloride raises the pitting potential.
3. The smaller the ionic radius, the more activity in the initiation step of pitting. The occurrence frequency of metastable pits, λ, has the most value in chloride bearing solution compared with NaBr and NaI solutions. λ severely increases in the mixed solution of NaF and NaCl to values even higher than NaCl solution.
4. The fastest metastable growth pertains to the NaCl solution. NaBr and NaI solutions respectively stand in second and third places, maybe because of more difficult diffusion in longer anionic radius.
5. Although the pitting is more probable in NaCl solution, its corresponding stability product is equal to that for NaI, NaBr and NaF + NaCl solutions or even lower in some cases.
6. Fluoride has a two-sided effect on the pitting. Its synergistic effect is to increase pitting nucleation when it is present alongside with chloride. On the other hand, as a component of a weak acid it has an inhibition effect for the propagation step of pitting. Consumption of protons by fluoride lowers the critical current density, hinders the pitting and raises the pitting potential.

References

[1] A.J. Sedriks, Corros. Stainless Steels (1996).
[2] G.S. Frankel, Pitting corrosion of metals, J. Electrochem. Soc. 145 (1998) 2186.
[3] M.G. Alvarez, J.R. Galvele, Shreir's Corrosion, Elsevier, 2010.
[4] J. Stewart, D.E. Williams, The initiation of pitting corrosion on austenitic stainless steel: on the role and importance of sulphide inclusions, Corros. Sci. 33 (1992) 457–474.
[5] D.E. Williams, M.R. Kilburn, J. Cliff, G.I.N. Waterhouse, Composition changes around sulphide inclusions in stainless steels, and implications for the initiation of pitting corrosion, Corros. Sci. 52 (2010) 3702–3716.
[6] D.E. Williams, J. Stewart, P.H. Balkwill, The nucleation, growth and stability of micropits in stainless steel, Corros. Sci. 36 (1994) 1213–1235.
[7] A.S.M. Paroni, N. Alonso-Falleiros, R. Magnabosco, Sensitization and pitting corrosion resistance of ferritic stainless steel aged at 800 °C, Corrosion 62 (2006) 1039–1046.
[8] G.T. Burstein, S.P. Vines, Repetitive nucleation of corrosion pits on stainless steel and the effects of surface roughness, J. Electrochem. Soc. 148 (2001) B504.
[9] P.C. Pistorius, G.T. Burstein, Metastable pitting corrosion of stainless steel and the transition to stability, Philos. Trans. R. Soc. A Math. Phys. Eng. Sci. 341 (1992) 531–559.
[10] J.R. Galvele, Transport processes and the mechanism of pitting of metals, J. Electrochem. Soc. 123 (1976) 464.
[11] F. Assaf, S. Abd El-Rehiem, A. Zaky, Pitting corrosion of zinc in neutral halide solutions, Mater. Chem. Phys. 58 (1999) 58–63.
[12] E. McCafferty, Sequence of steps in the pitting of aluminum by chloride ions, Corros. Sci. 45 (2003) 1421–1438.
[13] S.S. Abdel Rehim, H.H. Hassan, M.A. Amin, Chronoamperometric studies of pitting corrosion of Al and (Al–Si) alloys by halide ions in neutral sulphate solutions, Corros. Sci. 46 (2004) 1921–1938.
[14] M. Janik-Czachor, Effect of halide ions on the nucleation of corrosion pits in iron, Mater. Corros. 30 (1979) 255–257.
[15] E.A. Abd El Meguid, N.A. Mahmoud, Inhibition of bromide-Pitting corrosion of type 904L stainless steel, Corrosion 59 (2003) 104–111.
[16] B.R. Tzaneva, L.B. Fachikov, R.G. Raicheff, Effect of halide anions and temperature on initiation of pitting in Cr–Mn–N and Cr–Ni steels, Corros. Eng. Sci. Technol. 41 (2006) 62–66.
[17] A. Pardo, M.C. Merino, E. Otero, M.D. López, M.V. Utrilla, Pitting and crevice corrosion behaviour of high alloy stainless steels in chloride-fluoride solutions, Mater. Corros. 51 (2000) 850–858.
[18] J.M. Bastidas, C. Fosca, B. Chico, E. Otero, Corrosion behaviour of highly alloyed stainless steels in mixed chloride and fluoride aqueous solutions, Mater. Corros. 48 (1997) 216–220.
[19] O. Yamazaki, Effect of fluoride ion on the crevice corrosion for type 304 stainless steel in neutral NaCl solution, Zairyo-to-Kankyo 45 (1996) 365–369.
[20] M. Kaneko, H.S. Isaacs, Effects of molybdenum on the pitting of ferritic- and austenitic-stainless steels in bromide and chloride solutions, Corros. Sci. 44 (2002) 1825–1834.
[21] M. Kaneko, H.S. Isaacs, Pitting of stainless steel in bromide, chloride and bromide/chloride solutions, Corros. Sci. 42 (2000) 67–78.
[22] J.R. Davis, Stainless Steels, A.S.M. International, 1994.
[23] M.F. McGuire, Stainless Steels for Design Engineers, ASM International, 2008.
[24] I. Taji, M.H. Moayed, M. Mirjalili, Correlation between sensitisation and pitting corrosion of AISI 403 martensitic stainless steel, Corros. Sci. 92 (2015) 301–308.
[25] K.M. Zwilsky, Volume 1: Properties and Selection: Irons, Steels, and High-Performance Alloys, ASM Handb. (1993) 2071.
[26] A. Abbasi Aghuy, M. Zakeri, M.H. Moayed, M. Mazinani, Effect of grain size on pitting corrosion of 304L austenitic stainless steel, Corros. Sci. 94 (2015) 368–376.
[27] E.O. Nunez Moran, 2010. MSc Thesis, Evaluation of the Localized Corrosion Resistance of 21Cr Stainless Steels.
[28] D.E. Williams, Stochastic models of pitting corrosion of stainless steels, J. Electrochem. Soc. 132 (1985) 1796.
[29] T. Shibata, 1996 W.R. Whitney award lecture: statistical and stochastic approaches to localized corrosion, Corrosion 52 (1996) 813–830.
[30] J.R. Galvele, S.M. de De Micheli, Mechanism of intergranular corrosion of Al-Cu alloys, Corros. Sci. 10 (1970) 795–807.
[31] R.C. Newman, M.A.A. Ajjawi, H. Ezuber, S. Turgoose, An experimental confirmation of the pitting potential model of galvele, Corros. Sci. 28 (1988) 471–477.
[32] M.H. Moayed, R.C. Newman, Evolution of current transients and morphology of metastable and stable pitting on stainless steel near the critical pitting temperature, Corros. Sci. 48 (2006) 1004–1018.
[33] P.C. Pistorius, G.T. Burstein, Aspects of the effects of electrolyte composition on the occurrence of metastable pitting on stainless steel, Corros. Sci. 36 (1994) 525–538.
[34] G.S. Frankel, L. Stockert, F. Hunkeler, H. Boehni, Metastable pitting of stainless steel, Corrosion 43 (1987) 429–436.
[35] M. Ghahari, D. Krouse, N. Laycock, T. Rayment, C. Padovani, M. Stampanoni, F. Marone, R. Mokso, A.J. Davenport, Synchrotron X-ray radiography studies of pitting corrosion of stainless steel: extraction of pit propagation parameters, Corros. Sci. 100 (2015) 23–35.
[36] R.J. BRIGHAM, E.W. TOZER, Effect of alloying additions on the pitting resistance of 18% Cr austenitic stainless steel, Corrosion 30 (1974) 161–166.
[37] E. McCafferty, Introduction to Corrosion Science, Springer Science & Business Media, 2010.
[38] R.P. Bell, The Proton in Chemistry, Springer US, Boston MA, 1973.